Supplementary Information (SI) for Lab on a Chip.

Supplementary Material for

"Fully Printed and Flexible Patch for Real-Time Wireless Monitoring of Sweating Rate with Physiological Detecting"

Hao Wen[a], Kailong Dong[b], Feiyang Huang[a], Zhiqing Gao[a], Zijian An[a], Rujing Sun[a], Xin Li[a], Qing Ye[b] and Qingjun Liu*[ab]

[a] Biosensor National Special Laboratory, Key Laboratory for Biomedical Engineering of Education Ministry, Department of Biomedical Engineering, Zhejiang University, Hangzhou, 310027, P. R. China

[b] College of Computer Science, Jiangxi University of Chinese Medicine, Nanchang, 330004, P. R. China

* Corresponding Author: Qingjun Liu

E-mail address: qjliu@zju.edu.cn (Q. Liu).

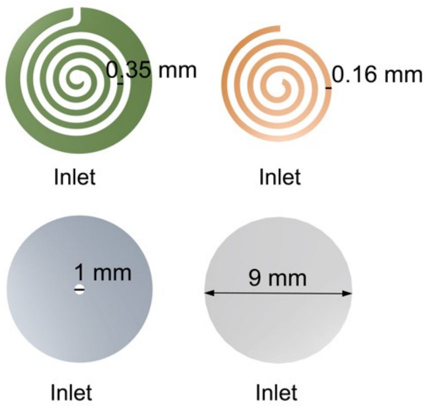

Figure S1. The structure and dimensions of each layer of the sweat sensor.

Figure S2. Fabrication process of polyurethane biocompatible substrate.

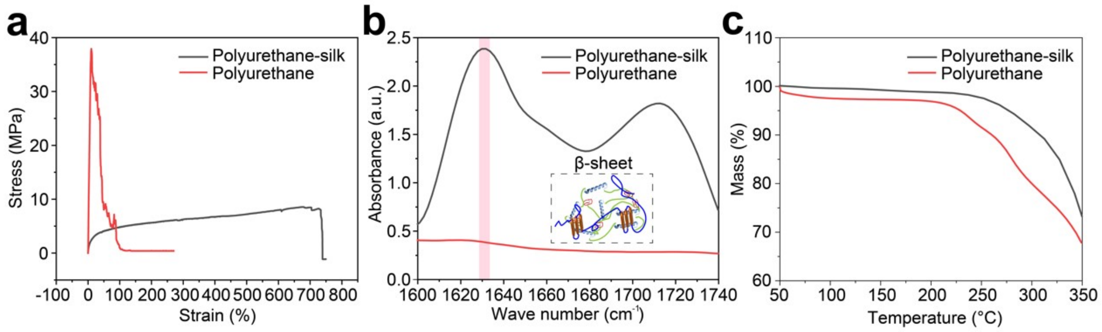

Figure S3. Comparison of performance characterization of polyurethane-silk film and polyurethane film. (a) Stress-strain curve. (b) Fourier transform infrared spectroscopy (FTIR). (c) Thermogravimetric curve.

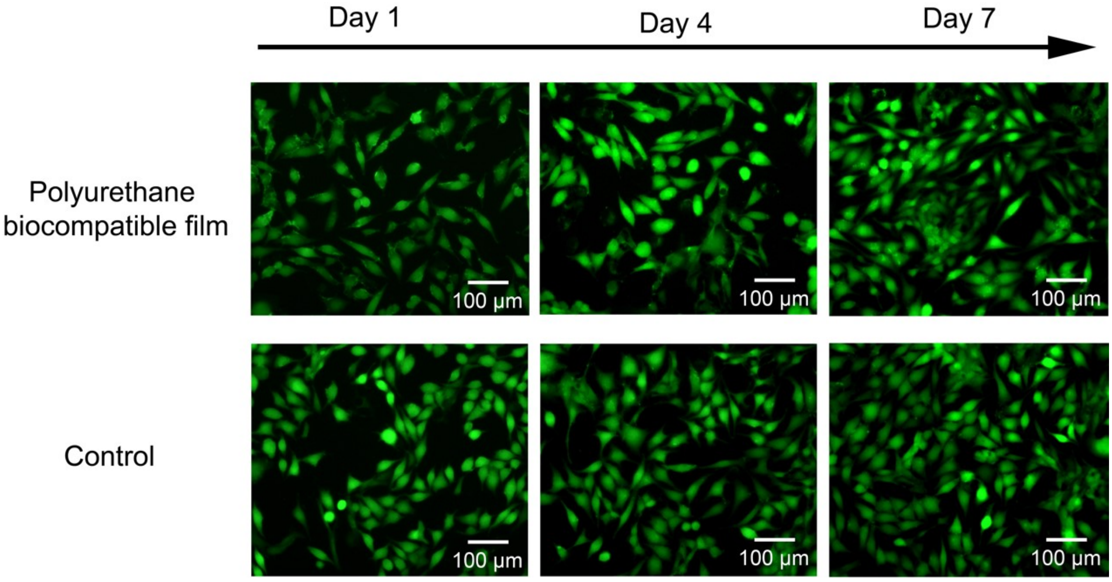

Figure S4. Experimental results of biocompatibility of mouse fibroblasts (L-929).

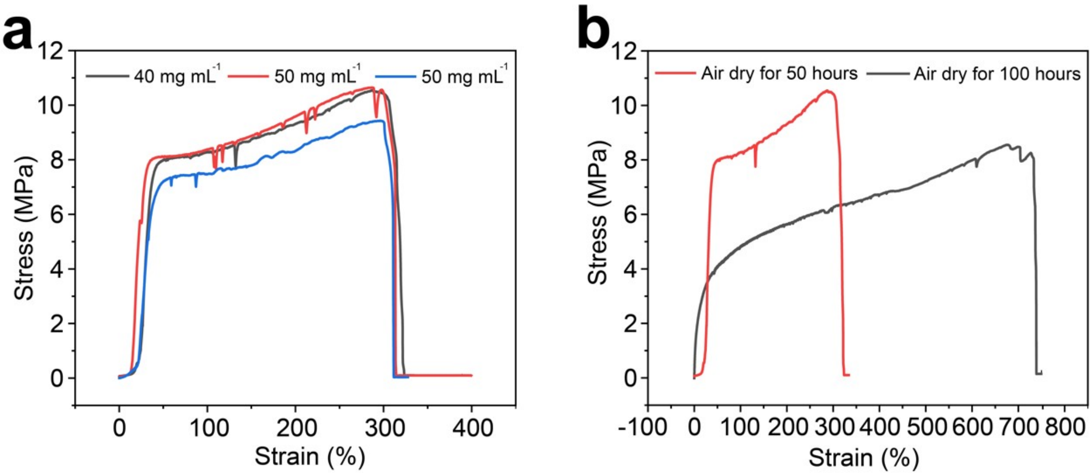

Figure S5. The influence of PU concentration and air-drying time on the mechanical properties of polyurethane silk substrate.

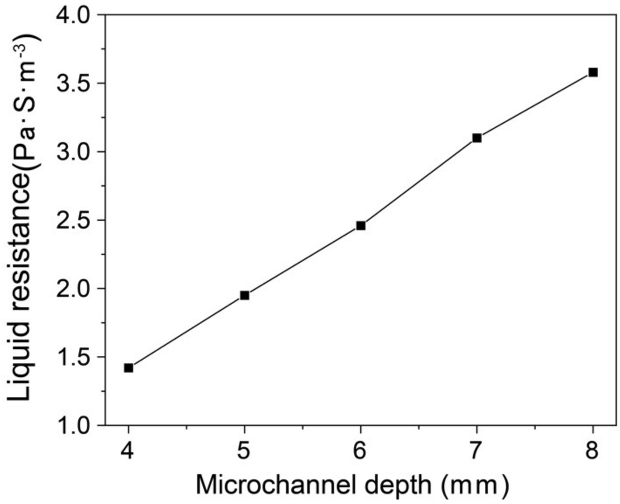

Figure S6. The linear relationship between flow channel depth and liquid resistance.

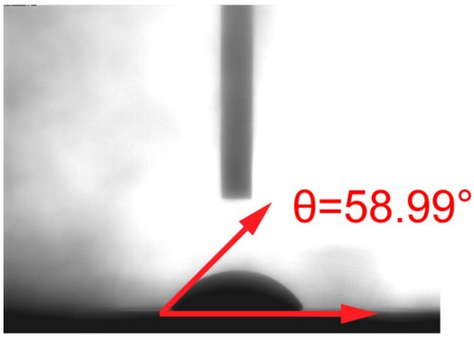

Figure S7. Contact Angle test of ink.

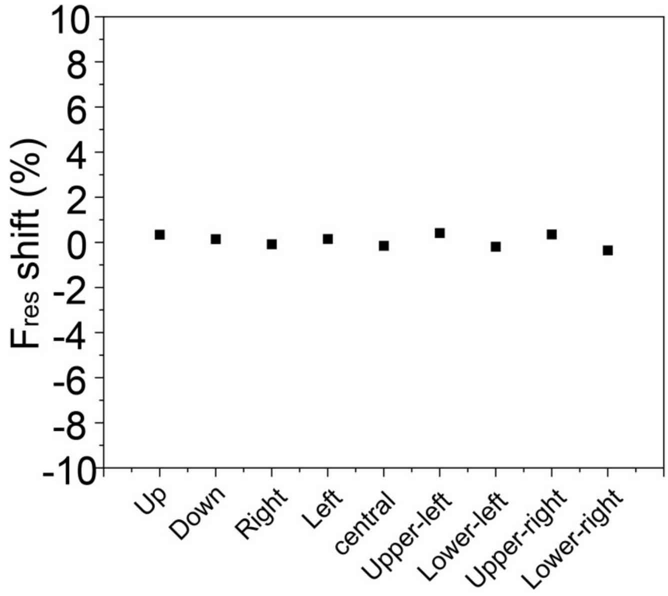

Figure S8. The influence of the relative positional orientation between the reader and the sensor.

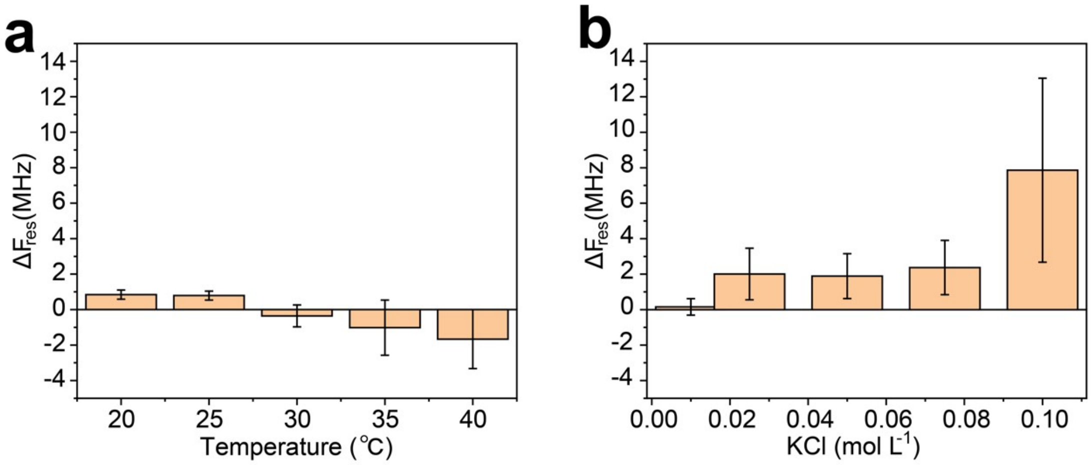

Figure S9. The influence of temperature and KCl concentration on the sensor's radio frequency signal.

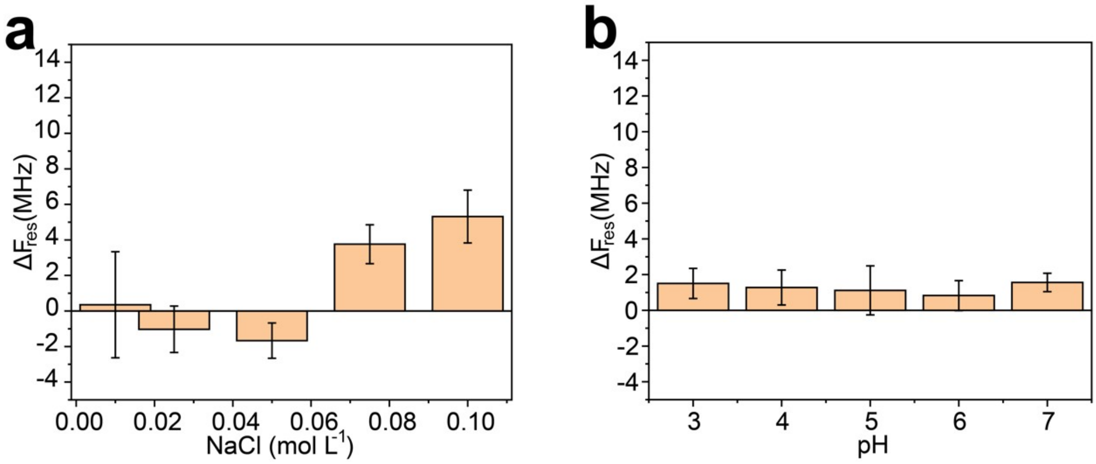

Figure S10. The influence of NaCl concentration and pH on the sensor's radio frequency signal.

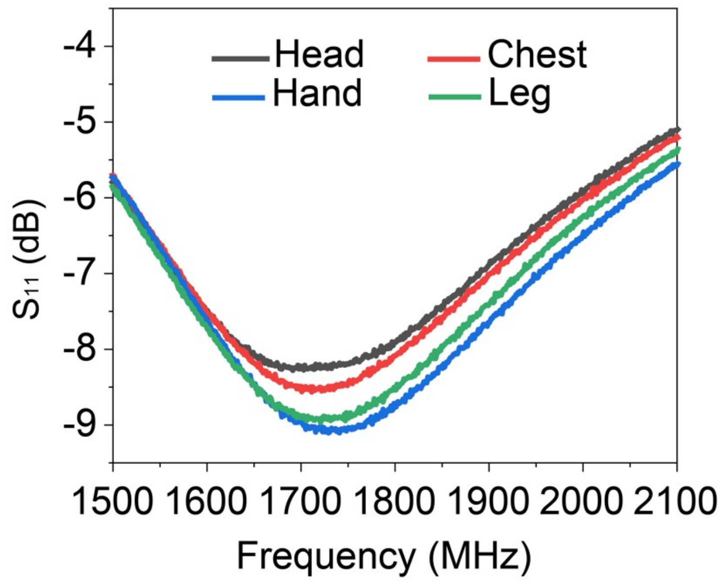

Figure S11. The offset of F_{res} when the sensor is placed at different positions.

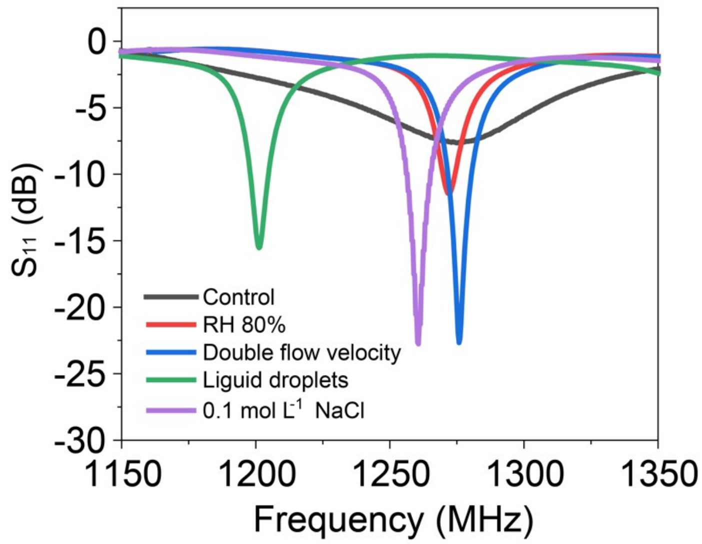

Figure S12. The effect of humidity, evaporation, sweating rate, ionic strength (NaCl level of sweat) on the F_{res}.

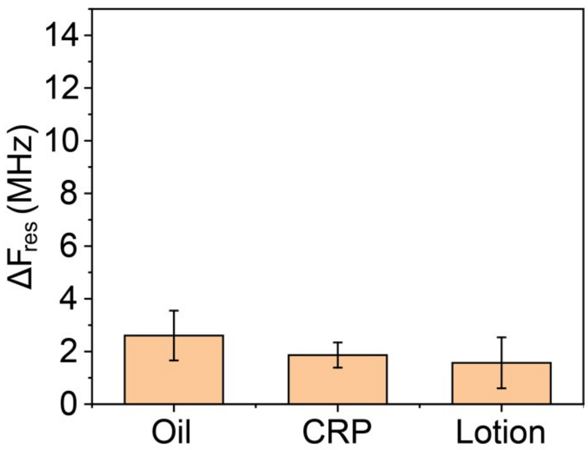

Figure S13. The influence of oil, protein and lotion on the sensor's radio frequency. Olive oil, CRP (C-reactive protein), vaseline were selected as representative oils, proteins, lotion for testing.

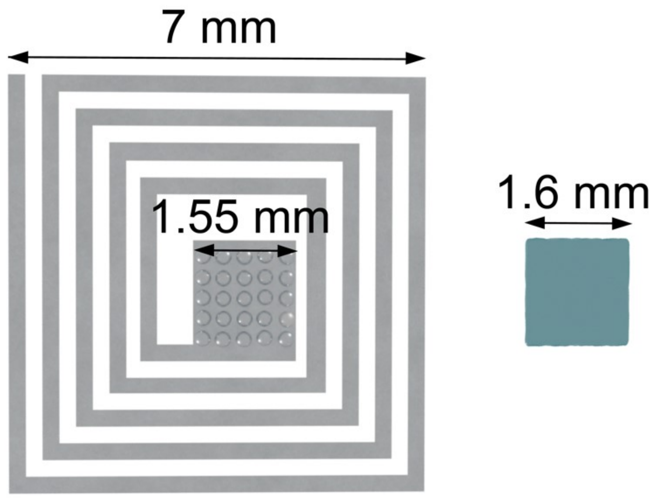

Figure S14. The structure and dimensions of each layer of the pressure sensor.

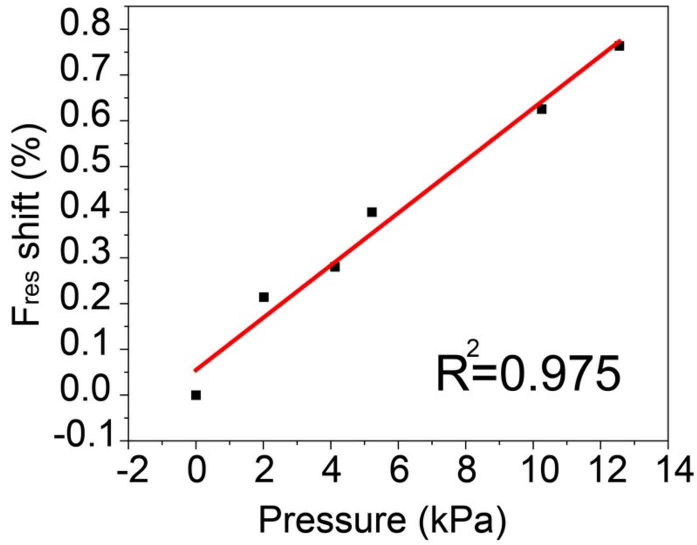

Figure S15. The linear relationship between the F_{res} shift and the applied pressure.

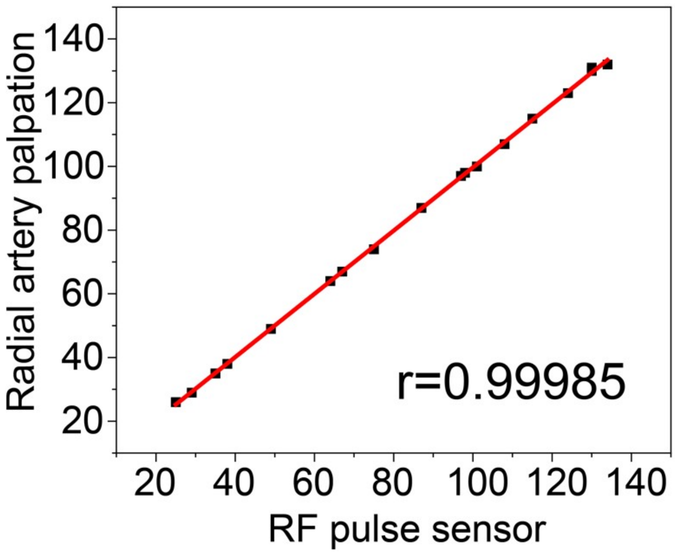

Figure S16. Comparison of the test results of arterial palpation and RF pulse sensor.

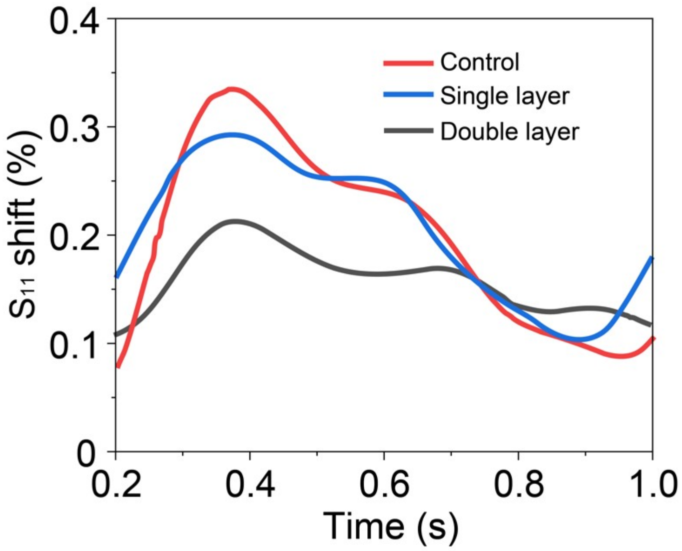

Figure S17. The influence of artificial skin on the pulse signal when it is separated between the skin and the RF pulse sensor.

Table S1. Comparisons between this work and other current works.

Methods	Bluetooth	Battery	Fully flexiblity	LoD (μL min^{-1})	Ref
Resistance	Yes	Yes	No	0.08	[1]
Capacitance	No	No	Yes	0.05	[2]
Resistance	No	Yes	Yes	0.5	[3]
Thermistor	Yes	Yes	Yes	/	[4]
Capacitance	Yes	Yes	No	0.42	[5]
Electrochemistry	Yes	Yes	No	0.025	[6]
Resistance	No	Yes	Yes	0.5	[7]
Resistance	No	Yes	Yes	0.1	[8]
Resistance	No	Yes	Yes	0.2	[9]
Resistance	Yes	Yes	Yes	/	[10]
Capacitance	No	No	Yes	0.04	This work

Notes and references

1. H. Y. Y. Nyein, L. C. Tai, Q. P. Ngo, M. H. Chao, G. B. Zhang, W. Gao, M. Bariya, J. Bullock, H. Kim, H. M. Fahad and A. Javey, *Acs Sensors*, 2018, **3**, 944-952.
2. D. H. Choi, M. Gonzales, G. B. Kitchen, D. T. Phan and P. C. Searson, *Acs Sensors*, 2020, **5**, 3821-3826.
3. L. Almulla, M. Mariello and C. M. Proctor, *Adv Funct Mater*, 2025, DOI: 10.1002/adfm.202510372.
4. K. Kwon, J. U. Kim, Y. J. Deng, S. R. Krishnan, J. Choi, H. Jang, K. H. Lee, C. J. Su, I. Yoo, Y. X. Wu, L. Lipschultz, J. H. Kim, T. S. Chung, D. R. Wu, Y. Park, T. I. Kim, R. Ghaffari, S. Lee, Y. G. Huang and J. A. Rogers, *Nat Electron*, 2021, **4**, 302-312.
5. A. Ria, M. Cicalini, P. Bruschi, M. Piotto and M. Dei, *Ieee Sens J*, 2025, **25**, 10250-10260.
6. M. A. Komkova, A. A. Eliseev, A. A. Poyarkov, E. V. Daboss, P. V. Evdokimov, A. A. Eliseev and A. A. Karyakin, *Biosens Bioelectron*, 2022, **202**.
7. S. Q. Wang, M. Y. Liu, X. Q. Yang, Q. F. Lu, Z. P. Xiong, L. H. Li, H. Zheng, S. M. Feng and T. Zhang, *Biosens Bioelectron*, 2022, **210**.
8. Y. Hashimoto, T. Ishihara, K. Kuwabara, T. Amano and H. Togo, *Micromachines-Basel*, 2022, **13**.
9. M. Y. Liu, S. Q. Wang, Z. P. Xiong, Z. Zheng, N. Ma, L. H. Li, Q. Gao, C. L. Ge, Y. F. Wang and T. Zhang, *Biosens Bioelectron*, 2023, **237**.
10. S. R. Kim, Y. F. Zhan, N. Davis, S. Bellamkonda, L. Gillan, E. Hakola, J. Hiltunen and A. Javey, *Nat Electron*, 2025, **8**.